JOURNAL OF VIROLOGY, July 2005, p. 8004–8013 Vol. 79, No. 13
0022-538X/05/$08.00+0 doi:10.1128/JVI.79.13.8004–8013.2005

Inhibition of Alpha/Beta Interferon Signaling by the NS4B Protein of Flaviviruses

Jorge L. Muñoz-Jordán,[1]† Maudry Laurent-Rolle,[1] Joseph Ashour,[1,2] Luis Martínez-Sobrido,[1] Mundrigi Ashok,[3] W. Ian Lipkin,[3] and Adolfo García-Sastre[1]*

Department of Microbiology[1] and Microbiology Graduate School Training Program,[2] Mount Sinai School of Medicine, New York, New York 10029, and Jerome L. and Dawn Greene Infectious Disease Laboratory, Mailman School of Public Health, Columbia University, New York, New York 10032[3]

Received 11 November 2004/Accepted 5 March 2005

Flaviviruses are insect-borne, positive-strand RNA viruses that have been disseminated worldwide. Their genome is translated into a polyprotein, which is subsequently cleaved by a combination of viral and host proteases to produce three structural proteins and seven nonstructural proteins. The nonstructural protein NS4B of dengue 2 virus partially blocks activation of STAT1 and interferon-stimulated response element (ISRE) promoters in cells stimulated with interferon (IFN). We have found that this function of NS4B is conserved in West Nile and yellow fever viruses. Deletion analysis shows that that the first 125 amino acids of dengue virus NS4B are sufficient for inhibition of alpha/beta IFN (IFN-α/β) signaling. The cleavable signal peptide at the N terminus of NS4B, a peptide with a molecular weight of 2,000, is required for IFN antagonism but can be replaced by an unrelated signal peptide. Coexpression of dengue virus NS4A and NS4B together results in enhanced inhibition of ISRE promoter activation in response to IFN-α/β. In contrast, expression of the precursor NS4A/B fusion protein does not cause an inhibition of IFN signaling unless this product is cleaved by the viral peptidase NS2B/NS3, indicating that proper viral polyprotein processing is required for anti-interferon function.

The arthropod-borne flaviviruses are important human pathogens. Dengue viruses (DEN) are the causative agents of the most prevalent insect-borne viral illness, dengue fever, characterized by high fever, chills, body aches, and skin rash. More than 50 to 100 million cases of dengue fever are reported yearly in over 80 countries where the mosquito vector *Aedes aegypti* is endemic, and approximately 500,000 patients suffer from the more debilitating and often lethal illnesses known as dengue hemorrhagic fever and dengue shock syndrome. Japanese encephalitis virus is the leading cause of arboviral encephalitis in Asia, accounting for 30,000 to 50,000 cases annually. St. Louis encephalitis virus causes sporadic epidemic encephalitis in the Americas. West Nile virus (WNV), previously unknown in the Western Hemisphere, has caused more than 9,000 cases in North America since 1999. Many infections are asymptomatic, and a small proportion of infected people develop a mild febrile syndrome; but 1% of cases are at a high risk of developing potentially fatal encephalitis. There is currently no specific treatment for dengue- and West Nile-related diseases or available vaccines to prevent human infection. The yellow fever virus (YFV) is largely under control due to the effectiveness of the yellow fever vaccine; nonetheless, the disease continues to occur intermittently in tropical South America and sub-Saharan Africa with a high fatality rate in infants.

Flaviviruses contain a positive-strand RNA molecule with a ≈10.7-kb-long open reading frame. After receptor-mediated endocytosis and release of the nucleocapsid in the cytoplasm (3, 18, 19), an interaction of ribosomes with the nucleocapsid brings the viral RNA to the cytoplasmic side of the rough endoplasmic reticulum (ER) (35, 36), where the RNA is translated into a polyprotein precursor (3,391 amino acids in the case of DEN). The polyprotein precursor is co- and posttranslationally processed by cellular and viral proteases acting in a sequential manner to yield three structural (C, prM, and E) and seven nonstructural (NS1, NS2A, NS2B, NS3, NS4A, NS4B, and NS5) proteins. The amino termini of prM, E, NS1, and NS4B are generated upon cleavage by the host ER signal peptidase in the ER lumen, whereas the NS2B/3 viral protease is responsible for the cleavage of most nonstructural proteins and the C terminus of the C protein in the cytoplasmic side of the ER (1, 2, 12). In addition, an unknown ER peptidase cleaves the C terminus of NS1 (11), and a furin protease produces a late cleavage of prM in the Golgi to generate the mature form of M protein (37). Positive- and negative-strand RNA molecules are replicated by the NS3/NS5 replicase complex in association with densely sedimenting membrane fractions (4, 39), which is followed by viral assembly and production of progeny.

The interferon (IFN) response ensues upon viral entry and release/synthesis of viral components, including double-stranded RNA intermediates that activate transcription factors such as interferon regulatory factor 3 (IRF-3), IRF-7, NF-κB, and ATF2/c-Jun. As a result, alpha/beta IFN (IFN-α/β) is transcribed (13, 33, 40–42). Secreted IFN-α/β binds to the IFN alpha receptor (IFNAR) on the surface of infected and neighboring cells, resulting in activation of the JAK/STAT pathway. Phosphorylated STAT1 and STAT2 recruit IRF-9 and activate

* Corresponding author. Mailing address: Department of Microbiology, Box 1124. Mount Sinai School of Medicine, 1 Gustave L. Levy Place, New York, NY 10029. Phone: (212) 241-7769. Fax: (212) 534-1684. E-mail: adolfo.garcia-sastre@mssm.edu.

† Present address: Centers for Disease Control and Prevention, Division of Vector-Born Infectious Diseases, Dengue Branch, 1324 Calle Cañada, San Juan, Puerto Rico 00920-3860.

IFN-stimulated regulatory elements (ISRE), promoting the expression of more than 100 genes (6). The fundamental role of IFN-α/β in protecting animal hosts against viral infections is most dramatically observed in mice deficient in the IFN pathway (10, 16, 27). In particular, IFNAR-deficient mice are extremely sensitive to DEN infection, exhibiting DEN replication in extraneural sites and subsequent viral spread into the central nervous system (34). In vitro studies had previously pointed to a protein kinase R-independent mechanism employed by infected cells to overcome DEN infections (7).

In establishing effective infections, viruses often overcome, at least in part, the onset of the innate antiviral response of the host cell. Importantly, the high pathogenicity of DEN in patients exhibiting high titers of IFN suggests that DEN antagonizes the IFN response in humans (21). The detailed mechanism employed by DEN to antagonize the IFN response has not been elucidated, but DEN infection had been shown to circumvent the action of IFN signaling in vitro (8). We have previously analyzed the ability of the 10 proteins encoded by DEN type 2 (DEN-2) to block the IFN system and found that expression of three of them results in partial inhibition of IFN-α/β signaling. Expression of NS4B strongly blocks the IFN-induced signal transduction cascade by interfering with STAT1 phosphorylation. NS4A and, to a lesser extent, NS2A also block IFN signaling, and the cumulative effect of the three proteins results in robust IFN signaling inhibition (28). Interestingly, the NS2A of Kunjin virus, a flavivirus closely related to WNV, has recently been described as an inhibitor of IFN-β production, indicating that the nonstructural proteins of flaviviruses target the IFN-α/β response at multiple levels (24). Here, we further explore the role of NS4B as an IFN antagonist and its functional conservation among other flaviviruses. We also report sequence requirements for the anti-IFN function displayed by DEN-2 NS4B in transfected cells. In addition, we find that the cleavage between NS4A and NS4B is required for their IFN antagonistic effect.

MATERIALS AND METHODS

Plasmid constructs, virus strains, and cell lines. The DEN-2 infectious cDNA clone pD2/IC-30P-A (20) served as a template for PCR amplification of DEN genes. All flavivirus genes and their truncations were cloned in the mammalian expression vector pCAGGS-COOH-TAG, a derivative of pCAGGS.MCS (29) containing the sequence 5′-CCCGGGATGTACCCTTATGATGTCCCAGATTATGCCTGACTCGAG-3′ cloned between SmaI and XhoI, encoding the hemagglutinin (HA)-TAG epitope YPYDVPDYA (underlined). pCAGGS-DEN-2 NS2B, NS3, NS4A, and NS4B have previously been described (28). For all DEN-2 NS4B mutant constructs that included the 2,000-molecular-weight (2K) segment, the forward primer (restriction sites highlighted in boldface) 5′-CCG**GAATTC**ACCATGGGAACACCCCAAGACAACCAACT-3′ was used. The reverse primers used for the NS4B truncations were the following (restriction sites in boldface): for $NS4B_{(1–232)}$, CC**GGTACC**GGTGGATTTCCTTCCCACAATGT; for $NS4B_{(1–155)}$, CC**GGTACC**GGTTCTCTGGTTGCTTTTGCTTG; for $NS4B_{(1–125)}$, **CCCGGG**GACTTGTGAGTAGCATCCAATGGC; for $NS4B_{(1–77)}$, **CCCGGG**ATGTCTCAACATTGGTGTAAC; and for $NS4B_{(1–47)}$, **CCCGGG**CTCGGGTTGCTGGGTTGCAATGC.

After PCR amplification, PCR products were cloned into pCAGGS-COOH-TAG by using EcoRI and KpnI [$NS4B_{(1–232)}$ and $NS4B_{(1–155)}$] or EcoRI and SmaI [$NS4B_{(1–125)}$, $NS4B_{(1–77)}$, and $NS4B_{(1–47)}$] restriction sites. To delete the 2K segment in Δ2KNS4B, the forward and reverse primers 5′-CCG**GAATTC**ACCATGAACGAGATGGGTTTCCTAGAAA-3′ and 5′-GG**GGTACC**CTTCTTGTGTTGGTTGTGT-3′, respectively, were used (restriction sites in boldface throughout). The following forward primer was used to replace the 2K segment of DEN-2 NS4B with the leader peptide of the murine major histocompatibility complex class I (MHC-I): 5′-CCG**GAATTC**ACCATGGTCCCGTGCACGCTGCTCCTGCTGTTGGCAGCCGCCCTGGCTCCTGGCTCCGACTCAGACCCGGGCCCGGAACGAGATG-3′. As a result, the following amino acid sequence was fused to the N-terminal of NS4B to replace the 2K segment by the murine MHC-I H-2KB (KB) leader peptide: MVPCTLLLLLAAALAPTQTRA. The DEN-2 NS4A/B region was amplified by PCR by using the forward primer 5′-CCG**GAATTC**ACCATGTCTCTGACCCTGAACCTAATCAC-3′ and the same reverse primer as the previous constructs. PCR products were cloned into pCAGGS-COOH-TAG between EcoRI and KpnI restriction sites. YFV NS4B was cloned by reverse transcription-PCR using RNA derived from the YF vaccine 17D by using the following primers: 5′-CCGG**ATCGAT**ACCATGTCCATCCAAGACAACCAAGTG-3′ and 5′-CC**GGTACC**GGCCGGCGTCCAGTTTTCATCTTC-3′. The amplified fragment was cloned in pGEM T-Easy vector (Promega), where site-directed mutagenesis was performed to produce the amino acid change E168K, present in wild-type YFV NS4B. The resulting cDNAs were inserted into pCAGGS-COOH-TAG between ClaI and KpnI restriction sites. WN NS4B (NY strain) was cloned using the primers 5′-GC**GAATTC**ACCATGCAACGTTCGCAGACAGACAAC-3′ and 5′-TACC**ATGCAT**CGTCTTTTTAGTCCTGGTTTTTCC-3′. The amplified fragment was cloned into pCAGGS-COOH-HA by using EcoRI and NsiI restriction sites. All flavivirus constructs were expressed with the HA-TAG epitope fused at their carboxy-terminals. The reporter plasmid pISRE-9-27-CAT (where CAT is chloramphenicol acetyltransferase) (40) was used for all CAT assays. Green fluorescent protein (GFP)-STAT1 was created by PCR amplification of STAT1 from pCMV-STAT1 (provided by J. Darnell) and cloning into a pCAGGS-derived version containing GFP. The firefly luciferase (FL) control plasmid (pCAGGS-FL) is also a pCAGGS-based plasmid. The construction and growth of the GFP-tagged Newcastle disease virus (NDV-GFP) is described elsewhere (30). Vero cells were obtained from the American Type Culture Collection and maintained in Dulbecco modified Eagle medium (DMEM) containing 10% fetal bovine serum (FBS).

Western blots. A total of 5×10^5 Vero cells were resuspended in 50 μl of loading buffer (100 mM Tris-ClH, pH 6.8, 200 mM dithiothreitol, 4% sodium dodecyl sulfate [SDS], 0.2% bromophenol blue, and 20% glycerol). Crude lysates were boiled for 10 min and then kept on ice. A total of 10 μl of each sample (equivalent to 5×10^5 cells) was loaded in a 12% polyacrylamide-SDS gel, and the proteins were electrophoretically separated by conventional methods. Proteins were transferred to nitrocellulose, and blots were blocked in 10% fat-free milk powder and 0.5% Tween 20 in phosphate-buffered saline (PBS). Incubations with anti-HA antibody (Sigma) were performed in 0.1% fat-free milk powder and 0.5% Tween 20 in PBS (incubation buffer) at 4°C overnight on a rotating platform. Blots were then washed three times for 10 min in incubation buffer, incubated for 1 to 2 h with goat anti-rabbit antibody (Amersham Bioscience), and washed three times for 10 min in incubation buffer and one time for 2 min in PBS. Antibody-protein complexes were detected using a Western Lighting chemiluminescence system (Perkin Elmer).

Reporter gene assays. Vero cells were transfected by using Lipofectamine 2000 (Invitrogen). Each transfection of 5×10^6 cells contained three plasmids: 1.2 μg of pISRE-9-27-CAT, 0.5 μg of pCAGGS-FL, and 5 μg of a pCAGGS construct of interest. At 24 h posttransfection, cells were mock treated or treated with 1,000 U of human IFN-β (Calbiochem). Cells were maintained in DMEM–10% FBS for 24 h posttreatment, and then cells were harvested and lysed. CAT assays were performed as previously described (31). Luciferase assays were performed by using a luciferase assay system (Promega).

Transfection and NDV-GFP infection of Vero Cells. Vero cells were transfected by using Lipofectamine 2000 (Invitrogen) as above. After 24 h of incubation at 37°C in DMEM–10% FBS, transfected cells were washed with PBS medium and incubated for 24 h more in the presence and in the absence of 1,000 U of IFN-β. Cells were then washed twice with PBS and infected with NDV-GFP at a multiplicity of infection of 1 to 2 at room temperature for 60 min. The inoculum was then aspirated, and cells were maintained in DMEM–10% FBS. The infected cells were incubated at 37°C prior to detection of GFP expression by fluorescence microscopy.

Immunofluorescence. Cells were grown on microscope coverslips and fixed and permeabilized in cold acetone:methanol (1:1). Cell nuclei were permeabilized for 5 min in 0.5% Nonidet P-40 (Sigma). HA-TAG mouse antibodies (Sigma) and rabbit polyclonal anti-calnexin (N and C terminus) (BD Biosciences) were used as primary antibodies. Texas red- and fluorescein isothiocyanate-conjugated anti-rabbit or anti-mouse (Jackson Immunochemicals) antibodies were used as secondary antibodies. Nuclear chromatin staining was performed by incubation in a PBS solution containing 0.5 mg/ml 4′,6-diamidino-2-phenylindole (DAPI; Sigma). Human IFN-β was used at 1,000U/ml in STAT1 induction studies.

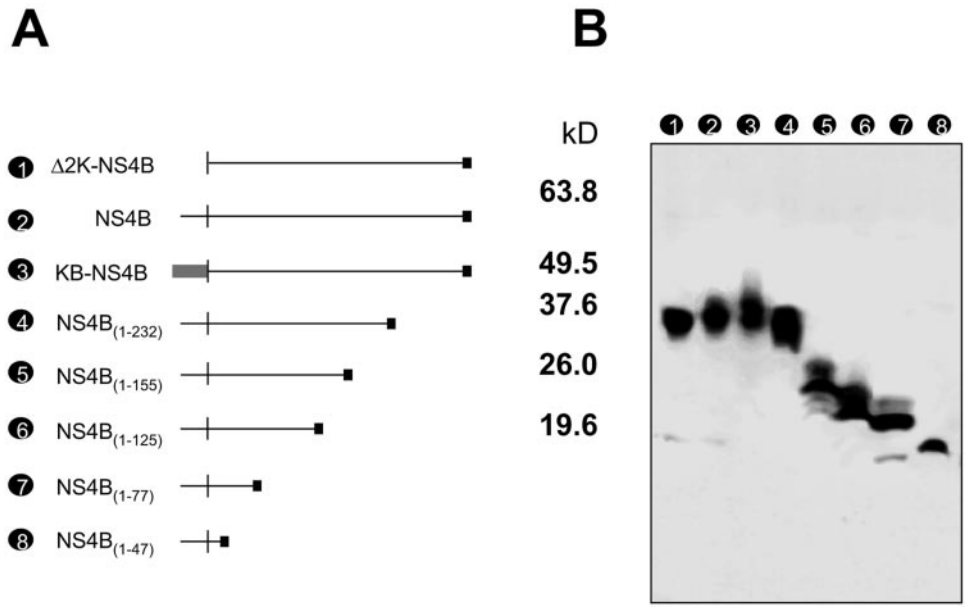

FIG. 1. Deletion analysis of DEN NS4B. (A) Schematic representation of various deletions of DEN-2 NS4B created by PCR. The N-terminal 2K segment was deleted (Δ2K-NS4B), left intact (NS4B), or replaced by the murine MHC-I signal peptide KB (KB-NS4B). In addition, deletions of the C-terminal region were also created by PCR [$NS4B_{(1–232)}$, $NS4B_{(1–155)}$, $NS4B_{(1–125)}$, $NS4B_{(1–77)}$, and $NS4B_{(1–47)}$] as indicated. (B) Immunoblot analysis of HA-tagged NS4B derivatives. All fragments represented in panel A were cloned in pCAGGS-HA to tag the C-terminal end of each protein. Expression levels of each protein were examined by running transfected cell extracts in a 4 to 20% gradient polyacrylamide. Proteins were transferred to a nitrocellulose membrane and detected with anti-HA primary antibody and horseradish peroxidase-labeled secondary antibody. Molecular mass (kDa) markers are at left.

RESULTS

A leader peptide is required at the N-terminal of DEN-2 NS4B for inhibition of IFN-α/β signaling. We have previously reported that expression of DEN-2 NS4B in transfected cells interferes with phosphorylation of STAT1 and activation of ISRE promoters after stimulation with IFN-α/β. To analyze the domains of DEN-2 NS4B necessary for this function, a series of partial deletions and substitutions in an NS4B expression plasmid was generated (Fig. 1A). All NS4B mutant proteins were HA tagged at the carboxy terminus. To check levels of expression, Vero cells were transfected, and crude protein extracts were electrophoretically separated in a 4 to 20% gradient polyacrylamide-SDS gel. The HA-tagged proteins were detected by immunoblotting using standard techniques (Fig. 1B). The results indicated that all proteins are expressed at comparable levels.

The ISRE-9-27 promoter is stimulated by IFN-α/β through the activation of the STAT1/STAT2/IRF-9 transcription factor (interferon-stimulated gene factor 3). This promoter is stimulated by IFN and not by virus-mediated activation of IRFs (5, 40). In order to investigate the ability of NS4B mutant proteins to inhibit IFN-mediated signal transduction, we studied ISRE-9-27 promoter activation in transfected Vero cells upon stimulation with exogenously added human IFN-β. Vero cells do not produce IFN (9), and therefore the IFN signaling detected is due only to stimulation by exogenous IFN. Each NS4B protein expression plasmid was transfected into Vero cells in combination with the ISRE-9-27-CAT reporter plasmid. Cells were incubated with IFN-β 24 h later, and cell lysates were prepared and assayed for CAT activity (Fig. 2A and 3A).

We first analyzed the possible contribution of the 2K segment to the IFN antagonistic function of NS4B. The 2K segment is a peptide 23 amino acids long that serves as signal peptide for the targeting of NS4B to the ER membrane. During viral infection, the 2K segment is cleaved at its amino terminus by the viral serine protease and subsequently on its carboxyl terminus by the host signal peptidase (22). We hypothesized that the absence of the 2K segment may cause incorrect targeting of NS4B in the ER membrane, rendering the molecule incapable of blocking IFN signaling. To test this, two NS4B mutants were generated: one lacking the 2K segment (Δ2K-NS4B) and a second with the murine MHC-I signal peptide KB substituting for the 2K segment (KB-NS4B). Each of these constructs was transfected into Vero cells together with the ISRE-9-27-CAT plasmid and pCAGGS-FL. After a 24-h stimulation with human IFN-β, CAT activity was measured and normalized with luciferase values. We found that the presence of Δ2K-NS4B in Vero cells did not inhibit IFN stimulation of ISRE-9-27 promoter. However, KB-NS4B blocked activation of the CAT reporter at levels similar to those of the wild-type NS4B. These results indicate that the anti-IFN function of NS4B depends on the presence of an N-terminal signal peptide. Because the sequence of this signal peptide is not specific, our data indicate that the 2K segment is not directly involved in blocking IFN-β. Expression and localization of Δ2K-NS4B and KB-NS4B were further analyzed by immunostaining. Unexpectedly, the results showed that all wild-type NS4B, Δ2K-NS4B, and KB-NS4B had similar patterns of localization and colocalized with calnexin, an ER marker protein (Fig. 2B). This suggests that the absence of the signal peptide

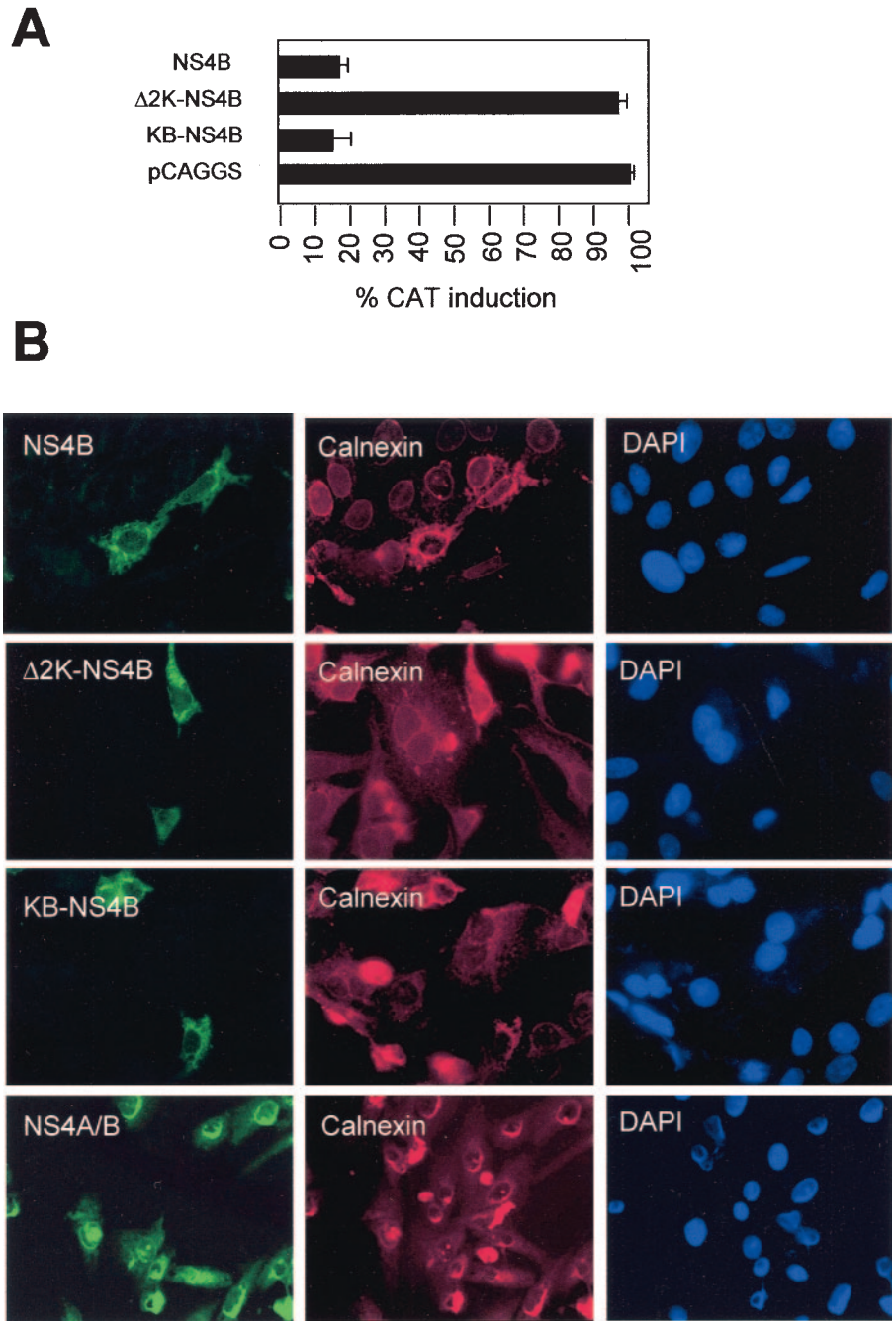

FIG. 2. Expression of 2K-mutant NS4Bs. (A) Induction of ISRE-9-27-CAT reporter gene after treatment with IFN. Recombinant pCAGGS-HA plasmids containing the DEN-2 NS4B, Δ2K-NS4B, or KB-NS4B gene fragments were transfected in Vero cells along with reporter plasmid ISRE-9-27-CAT and pCAGGS-FL. Following stimulation with 1,000 U of human IFN-β, CAT activity was quantitated in crude cell extracts. CAT activities were normalized to the corresponding FL activities to determine the percentage of CAT induction. CAT activities were determined as mean values from three independent experiments (*P* values of 0.02 to 0.06) (B) Immunostaining of transfected Vero cells. The indicated NS4B derivatives were expressed in Vero cells for 24 h. Cells were fixed, permeabilized, and immunostained using a polyclonal primary antibody for HA and a monoclonal anti-calnexin antibody. Fluorescein isothiocyanate-labeled secondary anti-rabbit antibody was used to detect NS4B proteins (green fluorescence) and a Texas red-labeled monoclonal antibody was used as a secondary antibody to detect calnexin (red fluorescence). DAPI staining reveals nuclear chromatin.

results in aberrant folding or topology of NS4B, rather than affecting ER targeting.

Analysis of domains in DEN-2 NS4B required for inhibition of IFN-α/β signaling. To determine the region of NS4B involved in its anti-IFN function, a carboxy-terminal deletion series of the protein was created (Fig. 1A). Upon expression of these truncated proteins in Vero cells and stimulation with human IFN-β, we measured CAT expression from the ISRE-

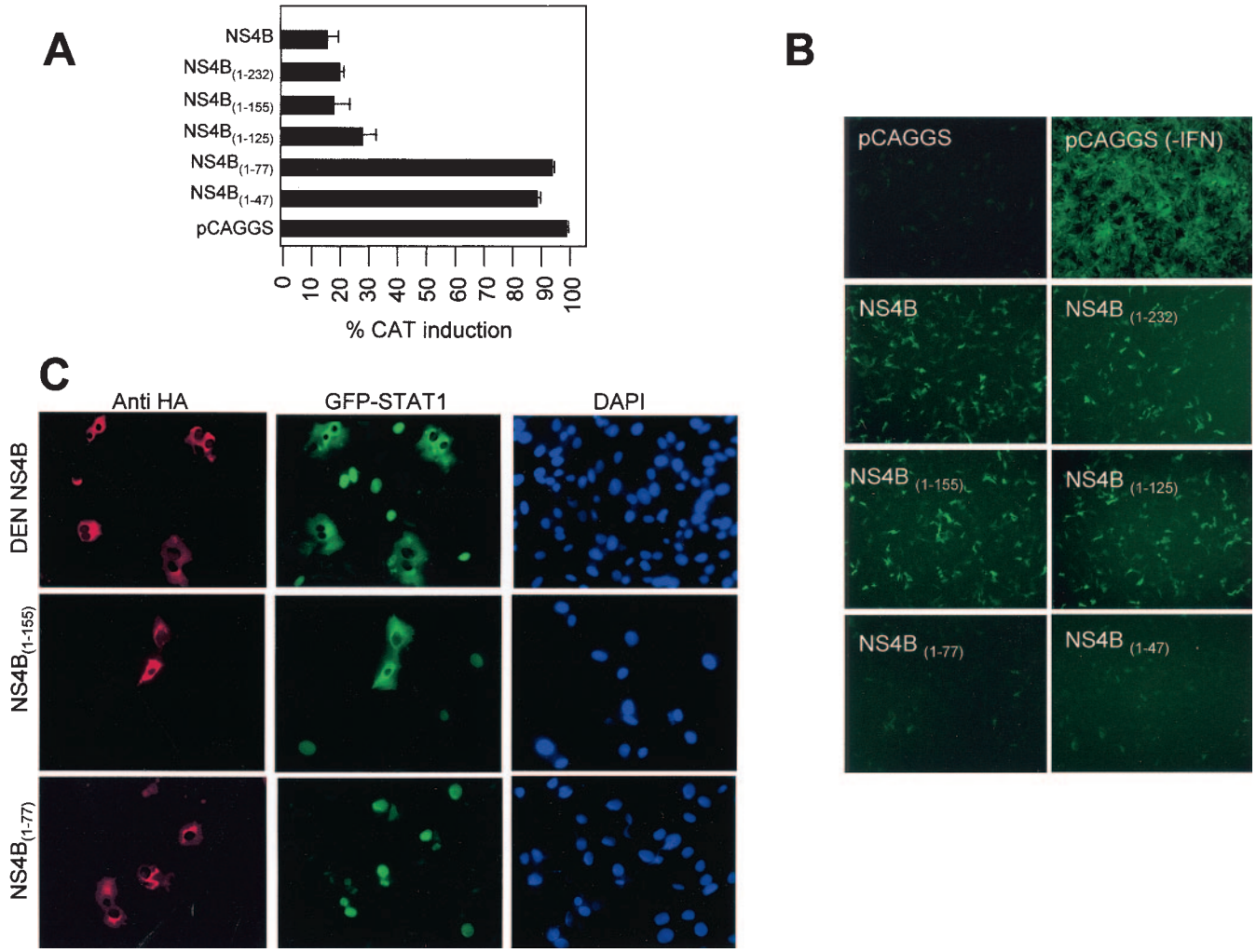

FIG. 3. Analysis of C-terminal deletions of DEN NS4B. (A) Induction of ISRE-9-27-CAT reporter gene after treatment with IFN. Recombinant pCAGGS-HA plasmids containing each of the DEN-2 NS4B C-terminal deletions were transfected in Vero cells together with the ISRE-9-27-CAT plasmid, and CAT expression was stimulated with 1,000 U of IFN-β 24 h later. Results show the percentage of CAT activity for each individual construct. CAT activities were determined as mean values from two independent experiments (*P* values of 0.01 to 0.05). (B) Inhibition of NDV-GFP replication by IFN in the presence of DEN-2 NS4B derivatives. Vero cells were transfected with the plasmids expressing the indicated NS4B wild-type and mutant proteins and stimulated with 1,000 U of IFN-β prior to infection with NDV-GFP. Expression of GFP was visualized as green fluorescence by fluorescence microscopy. (C) STAT1 activation by IFN in the presence of NS4B derivatives. Vero cells simultaneously expressing NS4B (red) derivatives and GFP-STAT1 (green) were stimulated with 1,000 U of human IFN-β for 35 min, fixed, and permeabilized. HA-labeled protein was detected by fluorescence microscopy after incubation with polyclonal antibodies to HA and Texas red-labeled secondary antibody.

9-27 reporter construct. The results showed that the domains of NS4B implicated in the block of IFN are located in the amino-terminal region of the protein (Fig. 3A). In particular, a truncated NS4B protein of 125 amino acids (including the 23 amino acids of the 2K segment) was still able to inhibit IFN signaling, while a further deletion of 48 amino acids [$NS4B_{(1–77)}$] rendered the protein incapable of blocking ISRE-9-27. Further deletion of the N terminus had similar effects. These results indicate that amino acid residues located between amino acids 77 and 125 in DEN-2 NS4B play an essential role in the inhibition of IFN signaling.

To confirm the IFN-signaling inhibitory properties, we next analyzed the ability of the different truncated NS4B proteins to promote viral replication in the presence of IFN. Vero cells were transfected with the mutant NS4B expression plasmids. After 24 h, the transfected cells were stimulated with human IFN-β. After an additional 24 h, the cells were infected with a Newcastle disease virus expressing GFP (NDV-GFP) and visualized by immunofluorescence microscopy (Fig. 3B). As expected, empty plasmid-transfected cells treated with IFN were not efficiently infected. In contrast, NDV-GFP replication was enhanced in IFN-treated Vero cells transfected with a plasmid expressing wild-type NS4B (272 amino acids in length, including the 2K segment). In addition, expression of the $NS4B_{(1–232)}$, $NS4B_{(1–155)}$, and $NS4B_{(1–125)}$ truncated proteins also resulted in enhanced NDV-GFP infection, indicating that amino acids 126 to 272 at the C-terminal of NS4B are not required for blocking IFN activity. However, further truncations of NS4B

eliminated the enhancement of NDV-GFP infection. These results correlate with the inhibition of ISRE promoter stimulation.

To further analyze the IFN-inhibitory properties of NS4B mutant proteins, we tested the ability of NS4B and its deletion series to block translocation to the nucleus of GFP-tagged STAT1. IFN-α/β binds to the cell surface receptor IFNAR, resulting in activation of JAK1 and TYK2 kinases, which then tyrosine phosphorylate STAT1 and STAT2, causing their heterodimerization and nuclear translocation. We have previously reported that NS4B blocks IFN-α/β-induced phosphorylation of STAT1 (28). We have tested the effects of NS4B in IFN-mediated translocation (activation) of STAT1 by transfecting Vero cells with NS4B expression plasmids together with a second plasmid expressing a GFP-STAT1 fusion protein. After 24 h, cells were starved for 2 h and then incubated in complete medium with human IFN-β for 35 min. HA antibody binding (indicative of expression of NS4B) and GFP signal were visualized in the fluorescence microscope (Fig. 3C). GFP-STAT1 was detected in the cytoplasm of cells expressing NS4B, whereas in cells not expressing NS4B, GFP-STAT1 was mostly present in the nucleus. Similarly, expression of the $NS4B_{(1–232)}$, $NS4B_{(1–155)}$, and $NS4B_{(1–125)}$ truncated proteins resulted in cytoplasmic retention of GFP-STAT1. However, in the presence of the $NS4B_{(1–77)}$ and $NS4B_{(1–47)}$ truncated proteins, GFP-STAT1 was mainly nuclear. Results are shown for wild-type NS4B, $NS4B_{(1–155)}$, and $NS4B_{(1–77)}$ (Fig. 3C). Collectively, our results indicate that the motifs required for the anti-IFN function of DEN-2 NS4B are present in the amino terminus of the protein and that critical candidate residues are located between amino acids 77 and 125.

Cleavage between NS4A and NS4B is required for IFN antagonism. We previously reported that expression of DEN-2 NS4A inhibits IFN-α/β signaling and that coexpression of NS4A and NS4B results in enhanced inhibitory activity (28). As all DEN polypeptides, NS4A and NS4B are expressed as part of the viral polyprotein. Two proteases are involved in the cleavage of NS4A and NS4B. The viral serine protease formed by NS2B and NS3 first cleaves the carboxyl terminus of NS4A; the host signal peptidase then cleaves the 2K segment, generating the amino terminus of NS4B. Cleavage by the viral peptidase is required prior to cleavage by the host signalase (22). To analyze the possible involvement of this particular cleavage mode in the IFN antagonistic functions of NS4A and NS4B, the entire NS4A/B region was cloned into the pCAGGS-COOH-TAG expression plasmid (Fig. 4A). To generate the two cleavage products NS4A and NS4B, we coexpressed NS2B and NS3 together with the NS4A/B fusion protein in Vero cells. The proteins in the crude cell extracts were electrophoretically separated in a 12% polyacrylamide-SDS gel. Immunoblotting revealed that the levels of expression of all proteins were comparable and that the cleavage by the viral peptidase generates NS4B (Fig. 4B). NS4B was visualized as a duplex band due to incomplete cleavage by the signal peptidase; this band is only observed if NS4B is expressed alone or if prior cleavage of NS4A/B by the viral peptidase has occurred.

In order to investigate the ability of NS4A and NS4B to block IFN signaling before and after cleavage, their ability to block activation of ISRE-9-27-CAT in the presence of IFN was analyzed (Fig. 4C). The results showed that in the absence of cleavage, the NS4A/B fusion protein did not block IFN-α/β induction of CAT expression, whereas the two proteins could strongly block such induction when they were expressed as individual polypeptides. Expression of the NS2B/NS3 viral protease restored the inhibition of IFN signaling when the NS4A/B fusion protein was also expressed. NS2B and NS3 did not exhibit antagonistic effects on their own. We further defined the anti-IFN function of these proteins by exploring their ability to block GFP-STAT1 translocation in response to IFN-α/β (Fig. 4D). We found that the NS4A/B fusion protein is only able to interfere with GFP-STAT1 translocation when coexpressed with NS2B and NS3. In summary, our results indicate that cleavage by the viral protease is required for the unfolding of the inhibition of IFN-α/β signaling by the DEN-2 NS4A and NS4B proteins. Interestingly, similarly to Δ2K-NS4B, the uncleaved NS4A/B fusion protein had a pattern of localization similar to that of NS4B and colocalized with calnexin, an ER marker protein (Fig. 2B, lower panels).

NS4B function is conserved among flaviviruses. Flavivirus genomes are conserved in their organization and sequence, with considerable amino acid sequence identity among them. In particular, DEN, YFV, and WNV are almost equally related to one another (42 to 49% amino acid sequence identity). NS4B is moderately conserved, with 30 to 36% amino acid sequence identity among these three flaviviruses. To explore the possible conservation of NS4B function in inhibiting IFN-α/β signaling, the YFV and WNV NS4B coding sequences were cloned into the pCAGGS-COOH-TAG expression plasmid. Crude protein extracts of transfected cells were electrophoretically separated in a 12% polyacrylamide-SDS gel, and an immunoblot showed that the proteins were expressed at levels comparable to those of their DEN homologue (Fig. 5A). Partial cleavage of the 2K segment by the host signalase was observed in DEN-2 and YFV NS4B proteins, whereas the WNV 2K segment was more efficiently cleaved. We then analyzed the ability of the three NS4B proteins to block IFN-induced activation of the ISRE-9-27 promoter using our CAT reporter system. The results clearly indicated that in Vero cells expressing NS4B of DEN, YFV, or WNV, activation of the ISRE-9-27 promoter in response to IFN-β is reduced to similar levels (Fig. 5B). In addition, cells expressing DEN, YFV, or WNV NS4B exhibited cytoplasmic retention of GFP-tagged STAT1 after IFN-β treatment (Fig. 5C and 3C, top panel). Taken together, our results demonstrate a conserved role of flavivirus NS4B proteins as inhibitors of IFN-α/β signaling.

DISCUSSION

We had previously reported that expression of DEN-2 NS4B and, to a lesser extent, NS4A and NS2A inhibited the activation of two different ISRE promoters in response to IFN-β. Coexpression of NS4A and NS4B resulted in a stronger block of ISRE-54 and ISRE-9-27 activation. The ability of NS4B to block IFN-β signaling was corroborated by the failure of cells expressing NS4B to activate (phosphorylate) endogenous STAT1 after stimulation with IFN-β (28). Here we have further defined the NS4B anti-IFN function by investigating its sequence requirements. We focused attention on NS4B because this protein exhibited the strongest inhibitory effect on

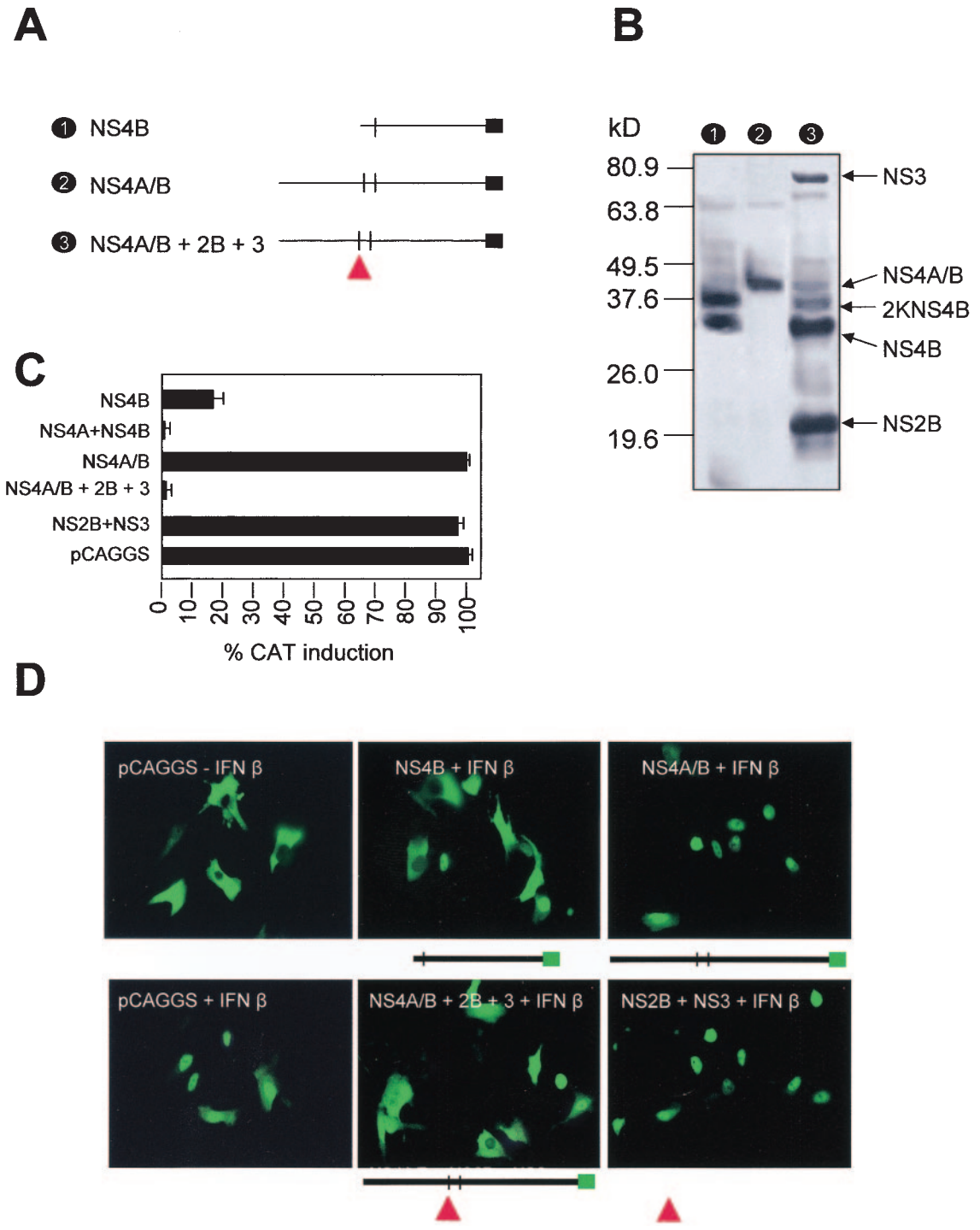

FIG. 4. Cleavage of NS4A/B. (A) Schematic representation of NS4A/B constructs. NS4A/B was derived by PCR and cloned in pCAGGS-HA. A schematic representation shows NS4B, NS4A/B, and NS4A/B in the presence of NS2B and NS3 (indicated by a triangle). (B) An immunoblot shows expression of these recombinant proteins in Vero cells. In the presence of NS2B and NS3, a complex pattern is obtained with bands coinciding with those obtained when only NS4B is transfected as indicated. Molecular mass markers (kDa) are at left. (C) Induction of ISRE-9-27-CAT after treatment with IFN. The percentage of CAT induction by IFN-β in the presence of the indicated expression plasmids is shown. CAT activities were determined as mean values from two independent experiments (*P* values of 0.03 to 0.05). (D) Activation of STAT1 by IFN in the presence of cleaved and uncleaved DEN proteins. GFP-tagged STAT1 protein was visualized by fluorescence microscopy in cells previously transfected with the indicated constructs and briefly stimulated with IFN-β. NS4A/B+2B+3, NS4A/B+NS2B+NS3. The presence of NS2B+NS3 is indicated by a triangle.

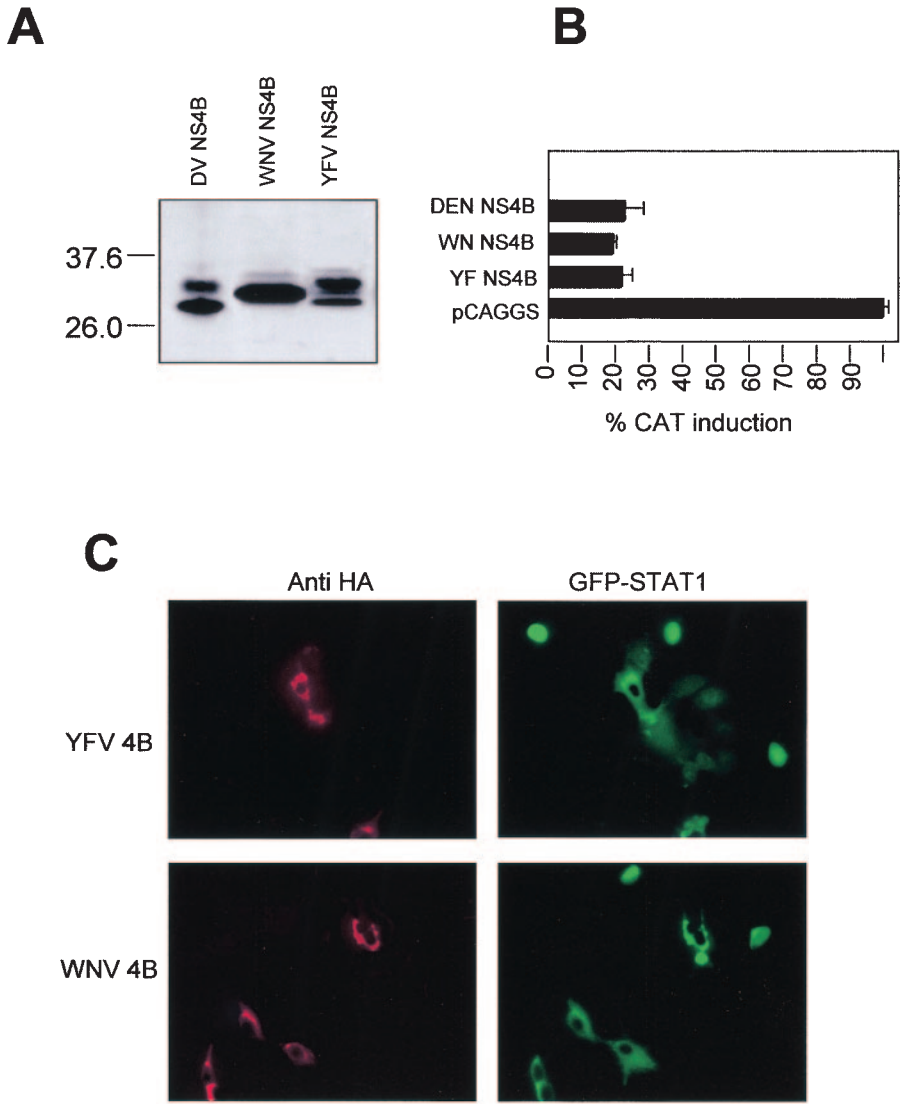

FIG. 5. Conserved NS4B function among flaviviruses. (A) An immunoblot shows levels of expression of DEN, WNV, and YFV NS4B in Vero cells transfected with the indicated plasmids. (B) Induction of ISRE-9-27-CAT after treatment with IFN-β. Vero cells were transfected with each of the indicated plasmids. At 24 h posttransfection, cells were treated with 1,000 U of human IFN-β. The CAT activities were normalized to the corresponding luciferase activities to determine CAT induction. CAT activities were determined as mean values from two independent experiments (*P* values of 0.02 to 0.04). (C) Vero cells simultaneously expressing YFV or WNV NS4B (red) and GFP-STAT1 (green) were treated with IFN-β. HA-labeled protein was detected by fluorescence microscopy after incubation with polyclonal antibodies to HA and Texas red-labeled secondary antibody.

ISRE activation (28). Our results indicate that the N-terminal 2K segment of NS4B, cleaved by the signal peptidase, is not directly involved in NS4B's anti-IFN function since its replacement by the murine MHC-I signal peptide KB resulted in an equally functional protein. However, lack of either signal peptide resulted in a nonfunctional NS4B protein, suggesting that these amino-terminal sequences are important for the correct insertion of NS4B in the ER membrane. After insertion, the leader peptide appears to be only partially removed (Fig. 5A). Therefore, we cannot ascertain at this moment whether both leader-peptide-containing and leader-peptide-cleaved NS4B proteins are functional inhibitors of IFN signaling.

To identify regions of NS4B responsible for this anti-IFN function, we performed deletions of the carboxy terminus and retained the integrity of the amino-terminal portion of NS4B. This strategy was used to minimize potential changes in the NS4B topology, which is predicted to be a membrane protein with multiple (five) membrane spanning domains (26, 32). We found that amino acid residues present between residues 77 and 125 are required for IFN antagonism. Interestingly, this area contains amino acids 77 to 103, which are predicted to be located in the cytoplasm between the first and the second transmembrane domains of NS4B. Thus, these amino acids are potentially implicated in interactions with cellular cytoplasmic components involved in IFN signaling. However, a careful experimental analysis of NS4B topology will be required in order to demonstrate the cytoplasmic localization of this domain of NS4B. It is attractive to speculate that this domain

might be involved in retaining the host cellular proteins required for IFN signaling, such as the JAK kinases, away from the plasma membrane, where activation of IFN signaling takes place through the IFN receptor. On the other hand, NS4B-mediated inhibition of IFN signaling might be an indirect effect achieved through the activation of cellular inhibitors of the JAK/STAT pathway. Future experiments are planned to address the mechanism of action of NS4B.

We also investigated the potential of the truncated DEN-2 NS4B proteins to inhibit STAT1 activation in response to IFN. We previously reported that IFN-β treatment of cells expressing NS4B did not result in detectable levels of tyrosine-phosphorylated (activated) STAT1 by immunofluorescence (28). Since STAT1 tyrosine phosphorylation is believed to mediate its nuclear accumulation, our previous results suggested that NS4B expression would result in inhibition of STAT1 nuclear translocation in response to IFN. We have confirmed this to be the case in Vero cells transfected with GFP-STAT1. This assay provides direct visualization of cytoplasmic and nuclear STAT1. Wild-type DEN-2 NS4B as well as all NS4B truncated proteins that inhibited reporter gene activation in response to IFN-β also inhibited STAT1 translocation.

Although the N-terminal signal peptide sequence of NS4B, the 2K segment, is processed by the signal peptidase of the host, cell-free in vitro translation studies had demonstrated that the NS4A/B region is cleaved by the host peptidase only after the N terminus of the 2K segment is cleaved by the NS2B-3 protease (22). Because NS4A and NS4B are both capable of blocking IFN signaling and together can produce a stronger antagonistic effect, we have studied the cleavage requirement for this function. We have found that the NS4A/B fusion protein is only able to inhibit IFN signaling when coexpressed with the viral protease. These data indicate that post-translational cleavage of the DEN-2 polyprotein is a prerequisite for activation of the IFN-antagonistic properties of NS4A and NS4B. If inhibition of IFN signaling is important for the pathogenicity of DEN in humans, viral protease inhibitors may be effective not only by interfering with the generation of viral products involved in viral RNA replication and virus assembly but also by indirectly interfering with the ability of DEN to inhibit the IFN-α/β antiviral system. Thus, we would predict that protease inhibitors would increase the sensitivity of DEN to the antiviral action of IFN-α/β. This prediction is reminiscent of the situation with the distantly related hepatitis C virus, in which it has been found that the viral protease contributes, albeit by a different mechanism, to the evasion of the IFN system by this virus (14).

The NS4B proteins of DEN, YFV, and WNV exhibit significant amino acid identity and block IFN signaling. The distantly related hepatitis C virus contains an NS4B gene with negligible sequence identity. Nonetheless, models of the predicted topology of NS4B, containing several ER and cytoplasmic domains separated by transmembrane regions, are significantly similar for the hepatitis C virus and other flaviviruses. Expression of NS4B of hepatitis C virus did not result in inhibition of IFN signaling in our assays (data not shown); however, other mechanisms have been implicated in inhibition of the IFN system by hepatitis C virus (14, 15, 38). Conservation of NS4B IFN antagonistic functions among flaviviruses suggests that this role of NS4B is important for efficient virus propagation. The ability of flaviviruses other than DEN to efficiently block IFN-α/β signaling was recently demonstrated. Japanese encephalitis virus appears to target the activation of the kinase Tyk2, essential for IFN signaling (23). Even more recently, Guo et al. (17) have found that West Nile virus replication inhibits IFN-α signaling by preventing JAK1 and Tyk2 activation, and Liu et al. (25) have shown that several nonstructural proteins of West Nile virus, including NS4B, inhibited STAT1/2 phosphorylation. These results are consistent with our observations described in the present study indicating that NS4B proteins from several flaviviruses have the ability to inhibit STAT1 activation and IFN signaling when individually overexpressed. It will be interesting to investigate whether similar or different mechanisms are used by different flaviruses to inhibit IFN signaling and whether this effect is dependent on NS4B. In addition, it is likely that inhibition of IFN signaling is required for viral replication and pathogenicity in the host. Thus, NS4B function represents a potential common target among flaviviruses for the development of new antiviral agents.

ACKNOWLEDGMENTS

This work was supported by grant U54 AI57158 (to A.G.-S and W.I.L.) from the National Institutes of Health and by a National Institutes of Health fellowship (to J.L.M.-J.). Microscopy was performed at the MSSM-Microscopy Shared Resource Facility, supported in part with funding from an NIH-NCI shared resources grant (R24 CA095823).

We thank J. Darnell for kindly providing the STAT1 cDNA. We also thank Maria Silva for the construction of the GFP-STAT1 plasmid and Richard Cádagan for excellent technical assistance.

REFERENCES

1. **Amberg, S., A. Nestorowicz, D. McCourt, and C. Rice.** 1994. NS2B-3 proteinase-mediated processing in the yellow fever virus structural region: in vitro and in vivo studies. J. Virol. **68:**3794–3802.
2. **Cahour, A., and B. Falgout.** 1992. Cleavage of the dengue virus polyprotein at the NS3/NS4A and NS4A/NS5 junctions is mediated by viral protease NS2B-NS3, whereas NS4A/NS4B may be processed by a cellular protease. J. Virol. **66:**1535–1542.
3. **Chen, Y., T. Maguire, and R. Marks.** 1996. Demonstration of binding of dengue virus envelope protein to target cells. J. Virol. **70:**8765–8772.
4. **Chu, P. W., and E. G. Westaway.** 1992. Molecular and ultrastructural analysis of heavy membrane fractions associated with the replication of Kunjin virus RNA. Arch. Virol. **125:**177–191.
5. **Deblandre, G. A., O. P. Marinx, S. S. Evans, S. Majjaj, O. Leo, D. Caput, G. A. Huez, and M. G. Wathelet.** 1995. Expression cloning of an interferon-inducible 17-kDa membrane protein implicated in the control of cell growth. J. Biol. Chem. **270:**23860–23866.
6. **Der, S., A. Zhou, B. Williams, and R. Silverman.** 1998. Identification of genes differentially regulated by interferon alpha, beta, or gamma using oligonucleotide arrays. Proc. Natl. Acad. Sci. USA **95:**15623–15628.
7. **Diamond, M., and E. Harris.** 2001. Interferon inhibits dengue virus infection by preventing translation of viral RNA through a PKR-independent mechanism. Virology **289:**297–311.
8. **Diamond, M., T. Roberts, D. Edgil, B. Lu, J. Ernst, and E. Harris.** 2000. Modulation of dengue virus infection in human cells by alpha, beta, and gamma interferons. J. Virol. **74:**4957–4966.
9. **Diaz, M., S. Ziemin, M. M. Le Beau, P. Pitha, S. Smith, R. Chilcote, and J. Rowley.** 1988. Homozygous deletion of the alpha- and beta 1-interferon genes in human leukemia and derived cell lines. Proc. Natl. Acad. Sci. USA **85:**5259–5263.
10. **Durbin, J., R. Hackenmiller, M. Simon, and D. Levy.** 1996. Targeted disruption of the mouse Stat1 gene results in compromised innate immunity to viral disease. Cell **9:**443–450.
11. **Falgout, B., and L. Markoff.** 1995. Evidence that flavivirus NS1-NS2A cleavage is mediated by a membrane-bound host protease in the endoplasmic reticulum. J. Virol. **69:**7232–7243.
12. **Falgout, B., M. Pethel, Y. Zhang, and C. Lai.** 1991. Both nonstructural proteins NS2B and NS3 are required for the proteolytic processing of dengue virus nonstructural proteins. J. Virol. **65:**2467–2475.
13. **Fitzgerald, K. A., S. M. McWhirter, K. L. Faia, D. C. Rowe, E. Latz, D. T.**

Golenbock, A. J. Coyle, S. M. Liao, and T. Maniatis. 2003. IKKepsilon and TBK1 are essential components of the IRF3 signaling pathway. Nat. Immunol. **4:**491–496.
14. **Foy, E., K. Li, C. Wang, R. Sumpter, M. Keda, S. Lemon, and M. Gale.** 2003. Regulation of interferon regulatory factor-3 by the hepatitis C virus serine protease. Science **300:**1145–1148.
15. **Gale, M., C. Blakely, B. Kwieciszewski, S. Tan, M. Dossett, N. Tang, M. Korth, S. Polyak, D. Gretch, and M. Katze.** 1998. Control of PKR protein kinase by hepatitis C virus nonstructural 5A protein: molecular mechanisms of kinase regulation. Mol. Cell. Biol. **18:**5208–5218.
16. **García-Sastre, A., R. Durbin, H. Zheng, P. Palese, R. Gertner, D. Levy, and J. Durbin.** 1998. The role of interferon in influenza virus tissue tropism. J. Virol. **72:**8550–8558.
17. **Guo, J. T., J. Hayashi, and C. Seeger.** 2005. West Nile virus inhibits the signal transduction pathway of alpha interferon. J. Virol. **79:**1343–1350.
18. **Heinz, F., G. Auer, K. Stiasny, H. Holzmann, C. Mandl, F. Guirakhoo, and C. Kunz.** 1994. The interactions of the flavivirus envelope proteins: implications for virus entry and release. Arch. Virol. **9**(Suppl.)**:**339–348.
19. **Heinz, F., K. Stiasny, G. Puschner-Auer, H. Holzmann, S. Allison, C. Mandl, and C. Kunz.** 1994. Structural changes and functional control of the tick-borne encephalitis virus glycoprotein E by the heterodimeric association with protein prM. Virology **198:**109–117.
20. **Kinney, R., S. Butrapet, G. Chang, K. Tsuchiya, J. Roehring, N. Bharapravati, and D. Gubler.** 1997. Construction of infectious cDNA clones of dengue virus: strain 16681 and its attenuated vaccine, strain PDK-53. Virology **230:** 300–308.
21. **Kurane, I., B. Innis, S. Nimmannitya, A. Nisalak, A. Meager, and F. Ennis.** 1993. High levels of interferon alpha in the sera of children with dengue virus infection. Am. J. Trop. Med. Hyg. **48:**222–229.
22. **Lin, C., S. Amberg, T. Chambers, and C. Rice.** 1993. Cleavage at a novel site in the NS4A region by the yellow fever virus NS2B-3 proteinase is a prerequisite for processing at the downstream 4A/4B signalase site. J.Virol. **67:** 2327–3335.
23. **Lin, R. J., C. L. Liao, E. Lin, and Y. L. Lin.** 2004. Blocking of the alpha interferon-induced Jak-Stat signaling pathway by Japanese encephalitis virus infection. J. Virol. **78:**9285–9294.
24. **Liu, W. J., H. B. Chen, X. J. Wang, H. Huang, and A. A. Khromykh.** 2004. Analysis of adaptive mutations in Kunjin virus replicon RNA reveals a novel role for the flavivirus nonstructural protein NS2A in inhibition of beta interferon promoter-driven transcription. J. Virol. **78:**12225–12235.
25. **Liu, W. J., X. J. Wang, V. V. Mokhonov, P. Y. Shi, R. Randall, and A. A. Khromykh.** 2005. Inhibition of interferon signaling by the New York 99 strain and Kunjin subtype of West Nile virus involves blockage of STAT1 and STAT2 activation by nonstructural proteins. J. Virol. **79:**1934–1942.
26. **Lundin, M., M. Monne, A. Widell, G. Von Heijne, and M. A. Persson.** 2003. Topology of the membrane-associated hepatitis C virus protein NS4B. J. Virol. **77:**5428–5438.
27. **Meraz, M., J. White, K. Sheehan, E. Bach, S. Rodig, A. Dighe, D. Kaplan, J. Riley, A. Greenlund, D. Campbell, K. Carver-Moore, R. DuBois, R. Clark, M. Aguet, and R. Schreiber.** 1996. Targeted disruption of the Stat1 gene in mice reveals unexpected physiologic specificity in the JAK-STAT signaling pathway. Cell **84:**431–441.
28. **Muñoz-Jordan, J., G. Sanchez-Burgos, M. Laurent-Rolle, and A. García-Sastre.** 2003. Inhibition of interferon signaling by dengue virus. Proc. Natl. Acad. Sci. USA **100:**14333–14338.
29. **Niwa, H., K. Yamamura, and J. Miyazaki.** 1991. Efficient selection for high-expression transfectants with a novel eukaryotic vector. Gene **108:**193–199.
30. **Park, M., M. Shaw, J. Muñoz-Jordán, J. Cros, T. Nakaya, N. Bouvier, P. Palese, A. García-Sastre, and C. F. Basler.** 2002. A Newcastle disease virus (NDV)-based assay demonstrates interferon-antagonist activity for the NDV V protein and the Nipah virus V, W, and C proteins. J. Virol. **77:**1501–1511.
31. **Percy, N., W. Barclay, A. García-Sastre, and P. Palese.** 1994. Expression of a foreign protein by Influenza A virus. J. Virol. **68:**4486–4492.
32. **Qu, L., L. K. McMullan, and C. Rice.** 2001. Isolation and characterization of noncytopathic pestivirus mutants reveals a role for nonstructural protein NS4B in viral cytopathogenicity. J. Virol. **75:**10651–10662.
33. **Sharma, S., B. R. tenOever, N. Grandvaux, G. P. Zhou, R. Lin, and J. Hiscott.** 2003. Triggering the interferon antiviral response through an IKK-related pathway. Science **300:**1148–1151.
34. **Shresta, S., J. Kyle, H. Snider, M. Basavapatna, P. Beatty, and E. Harris.** 2004. Interferon-dependent immunity is essential for resistance to primary dengue virus infection in mice, whereas T- and B-cell-dependent immunity are less critical. J. Virol. **78:**2701–2710.
35. **Singh, I., and A. Helenius.** 1992. Role of ribosomes in Semliki Forest virus nucleocapsid uncoating. J. Virol. **66:**7049–7058.
36. **Singh, I., M. Suomalainen, S. Varadarajan, H. Garoff, and A. Helenius.** 1997. Multiple mechanisms for the inhibition of entry and uncoating of superinfecting Semliki Forest virus. Virology **231:**59–71.
37. **Stadler, K., S. Allison, J. Schalich, and F. Heinz.** 1997. Proteolytic activation of tick-borne encephalitis virus by furin. J. Virol. **71:**8475–8481.
38. **Taylor, D., S. Shi, P. Romano, G. Barber, and M. Lai.** 1999. Inhibition of the interferon-inducible protein kinase PKR by HCV E2 protein. Science **285:** 107–110.
39. **Uchil, P., and V. Satchidanandam.** 2003. Architecture of the flaviviral replication complex. Protease, nuclease, and detergents reveal encasement within double-layered membrane compartments. J. Biol. Chem. **278:**24388–24398.
40. **Wathelet, M. G., C. Lin, B. S. Parekh, L. V. Ronco, P. M. Howley, and T. Maniatis.** 1998. Virus infection induces the assembly of coordinately activated transcription factors on the IFN-beta enhancer in vivo. Mol. Cell **1:**507–518.
41. **Weaver, B., K. Kumar, and N. Reich.** 1998. Interferon regulatory factor 3 and CREB-binding protein/p300 are subunits of double-stranded RNA-activated transcription factor DRAF1. Mol. Cell. Biol. **18:**1359–1368.
42. **Yoneyama, M., W. Suhara, Y. Fukuhara, M. Fukuda, E. Nishida, and T. Fujita.** 1998. Direct triggering of the type I interferon system by virus infection: activation of a transcription factor complex containing IRF-3 and CBP/p300. EMBO J. **17:**1087–1095.